

Microstructural and textural characterization of a hot-rolled IF steel

Jefferson Fabrício Cardoso Lins ·
Hugo Ricardo Z. Sandim · Hans-Jürgen Kestenbach

Received: 2 October 2006 / Accepted: 12 January 2007 / Published online: 30 April 2007
© Springer Science+Business Media, LLC 2007

Abstract The present paper reports the experimental results on the microstructural and textural characterization of a hot-rolled IF steel. The IF steel was hot-rolled in multiple passes in the austenitic field (1,070 °C) followed by air-cooling. SEM, TEM, and LOM were used to image the microstructure of the material. The global texture was determined by X-ray diffraction (XRD) technique. The mesotexture of selected regions was investigated by electron backscatter diffraction (EBSD). Results show the presence of a diffuse (nearly random) and weak texture in the hot-band that consists of recrystallized polygonal grains and subgrains. The fraction of boundaries with misorientations comprised in the interval $2^\circ \leq \psi < 15^\circ$ was found to be lower than 5%. It can be concluded that these low angle boundaries and the presence of subgrains can be associated to the existence of a few areas softened by recovery during or after hot rolling in austenitic field.

Introduction

One major role of texture studies in recent years has been in optimizing the recrystallization texture of IF-steel sheets for further deep-drawing operations. This material is targeted for the automotive industry, in particular in the manufacture of body panels. Particles of carbides and nitrides can be found in the microstructure as a result of the addition of the microalloying elements (Ti, Nb, and V). These elements tend to form stable compounds rather than being dissolved interstitially in ferrite. The compounds frequently found in the Ti-bearing IF steels consist mainly of TiN, TiS, $Ti_4C_2S_2$ and Ti (CN). The Ti-rich particles play an important role upon annealing retarding recovery and recrystallization in deformed austenite [1].

The absence of solute interstitial elements and the appropriate texture in IF steels leads to excellent deep-drawability. Many efforts have been undertaken to understand the microstructural evolution of cold-rolled low-carbon steels and their behavior during further annealing. The final recrystallization texture of IF steels is characterized by a strong and homogeneous $\{111\}\langle uvw \rangle$ fiber texture (γ -fiber) with a secondary component $\{554\}\langle 225 \rangle$ [2–4].

On the other hand, the texture found in hot bands of ultra-low carbon steels results from a complex combination of inhomogeneous plastic deformation, the occurrence of dynamic recovery and/or recrystallization during hot rolling, and the $\gamma \rightarrow \alpha$ phase transformation. The study of the hot rolling texture and microstructure of the IF-steels is necessary for a full description of the starting texture and its subsequent evolution during cold rolling and further annealing to develop the most suitable texture for further deep-drawing. For the local texture studies the application of EBSD coupled with orientation imaging microscopy

J. F. C. Lins (✉)
Escola de Engenharia Industrial Metalúrgica de Volta Redonda,
Universidade Federal Fluminense, Volta Redonda
RJ 27255-125, Brazil
e-mail: jfclins@metal.eeimvr.uff.br

H. R. Z. Sandim
Escola de Engenharia de Lorena, Universidade de São Paulo,
P.O. Box 116, Lorena, SP 12600-970, Brazil

H.-J. Kestenbach
Universidade Federal de São Carlos, Sao Carlos 13565-905,
Brazil

(OIM) is a powerful tool to understand the microstructural evolution and mesotexture relations [5].

In the present paper we report the experimental results on the microstructural and textural characterization of commercial Ti-stabilized IF steel. Information concerning the mesotexture of this material is rarely found in the literature. A new methodology for metallographic preparation of IF-steel was also proposed in this work. Light optical microscopy (LOM), scanning electron microscopy (SEM), and transmission electron microscopy (TEM) examinations were performed in the rolling plane and in transversal section. The distribution of degrees of misorientations (ψ) across boundaries between pairs of adjacent grains and the respective local texture of the material was evaluated using EBSD technique in representative areas. Macrotecture of polished samples was determined with the aid of conventional X-ray diffraction (XRD).

Experimental

Material

Companhia Siderúrgica Nacional (CSN, Brazil) has supplied the Ti-stabilized IF steel used in this investigation. The plate dimensions were 250 × 300 × 38 mm. This plate was obtained by hot rolling in multiple passes in the austenitic field down to 1,070 °C followed by air-cooling. The initial thickness of the steel plate was 257-mm. The chemical composition of this steel is shown in Table 1.

Metallography of IF steel

Metallographic preparation of the specimens was carried out using a new methodology to reveal the true microstructure. The samples were mounted in conducting Bakelite. Both polishing and etching operations performed in low carbon steels for EBSD analysis are usually based on electrolytic routes using hazardous HClO₄-containing solutions. In this work, we propose a simplified chemical-mechanical polishing route. First, the samples were ground with moderate pressure using SiC-emery papers up to 2,400-mesh. Commercial ethanol was used as lubricant. Semi-automatic polishing was the final step for preparation of the samples. A solution with 25 mL of OP-U colloidal silica (Struers), 1,975 mL of distilled water, 1 mL of nitric

acid and 10 mL of commercial neutral detergent was used as the polishing medium. The OP-CHEM (Struers) polishing hard and chemical resistant cloth was used in a Buehler semi-automatic machine (PHOENIX 4000V/1) at 300 rpm. In each sample a constant force of 35 N was applied during about 2 h with a flow rate of the polishing solution of 0.3 L/h. Chemical etching was done using a conventional Nital 3% acid solution at room temperature. The samples were etched by immersion during about 20 s to remove the surface deformation layer and reveal the true microstructure. This metallographic preparation has the advantage of being used for both microtexture and macrotecture evaluations.

Microstructural characterization

Light optical microscopy (LOM) images were acquired in a Leica DM IRM microscope with normal illumination (bright field). The measurements of grain size were performed by means of a semi-automatic routine for LOM using an automated image analysis system. The results obtained with the LOM routine were also compared with those determined using the EBSD technique. The semi-automatic routine for optical microscope was developed with Leica Q-Win 2.3 software. This routine was initially developed for fully recrystallized niobium sheets [6]. The image resolution was 640 × 480 pixels at magnification of 50 times. The measurements were made in 20 fields in the rolling plane and in the transversal section, respectively. For the image analysis routine, the Ti-IF steel was etched by immersion for about 70 s with Nital 3% after metallographic preparation to mark the presence of boundaries in the very clean ferritic matrix.

Electron channeling contrast images of Ti-bearing IF steel were carried out in a LEO 1450-VP scanning electron microscope operating at 10 kV in the backscattered electrons mode (BSE). This technique provides crystallographic contrast at low magnification and allows identifying regions with misorientations (ψ) around 2° or less by the variation in the gray scale in BSE images. TEM was carried out in JEOL JEM-100CX operating at 100 kV.

Microtexture and macrotecture evaluation

Orientation imaging maps were taken in six random areas. The fundamentals of this technique are given elsewhere

Table 1 Chemical composition of the Ti-stabilized IF steel (wt.%)

C	Mn	P	S	Si	N	O
0.003	0.172	0.011	0.005	0.011	0.0025	0.0054
Ni	Cr	Mo	Al	Nb	V	Ti
0.004	0.002	0.002	0.049	0.001	0.003	0.069

[7, 8]. The EBSD scans were carried out in areas of about $365 \times 1,340 \text{ } (\mu\text{m})^2$. For the rolling plane the step size in each scan (L1, L2 and L3) was $6 \text{ } \mu\text{m}$. Orientation maps (T1, T2 and T3) in the transversal section (i.e., plane containing transversal (TD) and normal (ND) directions) were performed with a step size of $7 \text{ } \mu\text{m}$. The grain size and microtexture of the IF steel plate were determined by means of automatic indexing of Kikuchi patterns after suitable image processing in a TSL system interfaced to a PHILIPS XL-30 scanning electron microscope operating at 30 kV with W-filament. Analysis of EBSD data was done in such a manner that any orientation-point pair with misorientation exceeding 2° was considered as a boundary. Smaller misorientations can not be resolved by this technique (intrinsic limitation) [8].

The macrotexture of the steel plate was determined in a RIGAKU model D/MAX-2000 diffractometer using a $\text{Mo } k\alpha_1$ ($\lambda = 0.7093 \text{ } \text{Å}$) radiation. Measurements of longitudinal, mid-thickness and transversal section were performed in samples with $15 \times 20 \times 10 \text{ mm}$.

Results and discussion

The true effective von Misses plastic strain (ϵ) after the hot rolling schedule was about 2.2. The literature reports that during this process, the parent phase (austenite) develops an enhanced and strong crystallographic texture which is later inherited by ferrite on transformation after air-cooling [1–3].

Figure 1 shows, respectively, the rolling plane and transversal sections of the material. These figures show the presence of polygonal grains resulting from the transformation of austenite into ferrite phase. Thus, the microstructure of the IF steel plate consists of a ferritic matrix and Ti-rich precipitates. The electron channeling contrast map shows low angle boundaries in a few areas (Fig. 2a) and the TEM micrograph clearly reveals the presence of subgrains and a few particles with sizes around $0.15 \text{ } \mu\text{m}$ (Fig. 2b). The average subgrain size from TEM is about $1 \text{ } \mu\text{m}$. The presence of this substructure strongly suggests the occurrence of recovery during hot rolling in some areas because the austenite was not able to recrystallize completely during or after the rolling as result the presence of titanium particles [3].

EBSD and a traditional method of quantitative metallography (LOM) were also used to evaluate the true grain size in the hot band. Table 2 displays the results of grain size determinations in longitudinal and transversal sections of the plate. The traditional quantitative metallography using LOM has the advantage of providing faster results than other techniques, including the linear intercept method by EBSD image analysis. It is worth mentioning that the

success of LOM routine strongly depends on careful metallographic preparation and is very dependent on the extent of the chemical etching. We observed a good agreement between results obtained from both techniques in the case of the transversal section. However, results of mean grain size in longitudinal section display a discrepancy of about $10 \text{ } \mu\text{m}$. The literature suggests a number close to 200 grains with 20,000 orientation-data points for the determination of grain size by EBSD [9]. In the case of the transversal section such statistics were satisfied (277 grains with 25,340 orientation-data points). However, only 16,800 points could be sampled in 293 grains in the rolling plane using a step size of $6 \text{ } \mu\text{m}$. The hot band has a grain size of $55 \pm 6 \text{ } \mu\text{m}$. This result agrees with others reported in the literature for IF-steel processed in a similar manner [10].

Figure 3 shows the $\{211\}$ pole figures corresponding to the longitudinal and transversal sections of the Ti-stabilized IF steel plate. The figure exhibits several isolated components with reasonable intensity distributed in pole figures, which is typical of a coarse-grained material. Thus, these results reveal the existence of a very weak or almost random texture in the plate independent of the section considered. In addition, it is worth mentioning that the textures displayed in the rolling plane (Fig. 3a) and the center layer (Fig. 3b) do not exhibit considerable differences in terms of components and intensity levels through

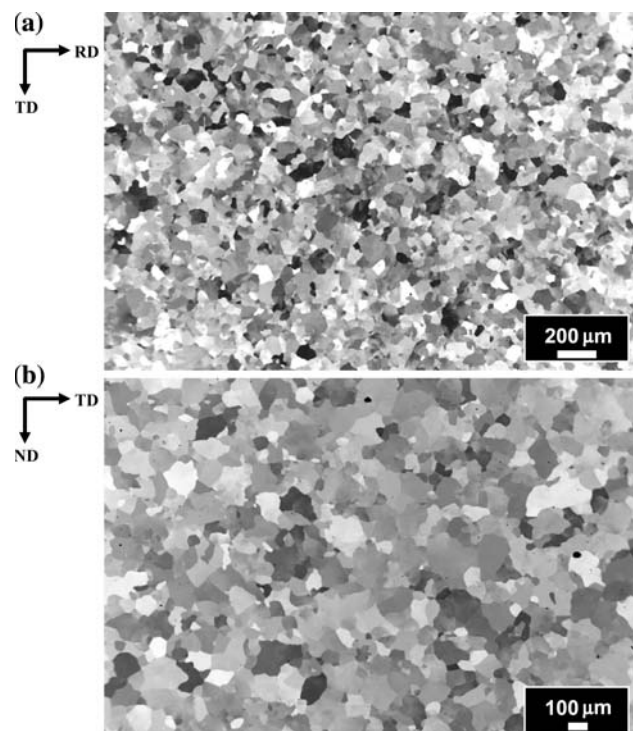


Fig. 1 Electron channeling contrast images of the IF steel plate: (a) rolling plane; (b) transversal plane. TD refers the transversal direction

Fig. 2 Micrographs showing details of the microstructure of IF steel plate: (a) electron channeling contrast image showing low angle boundaries (SEM–BSE, 10 kV), (b) subgrains (TEM, bright field—100 kV)

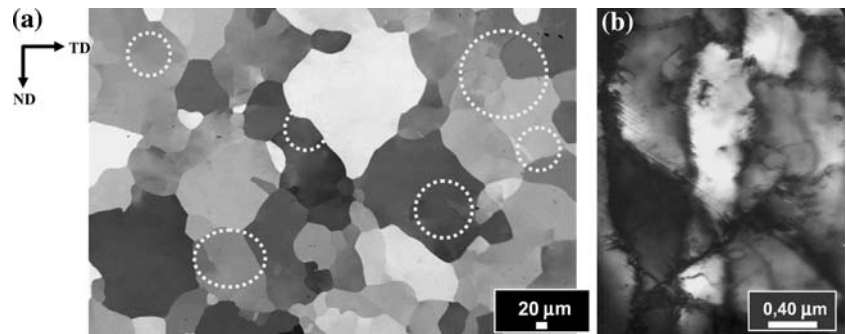
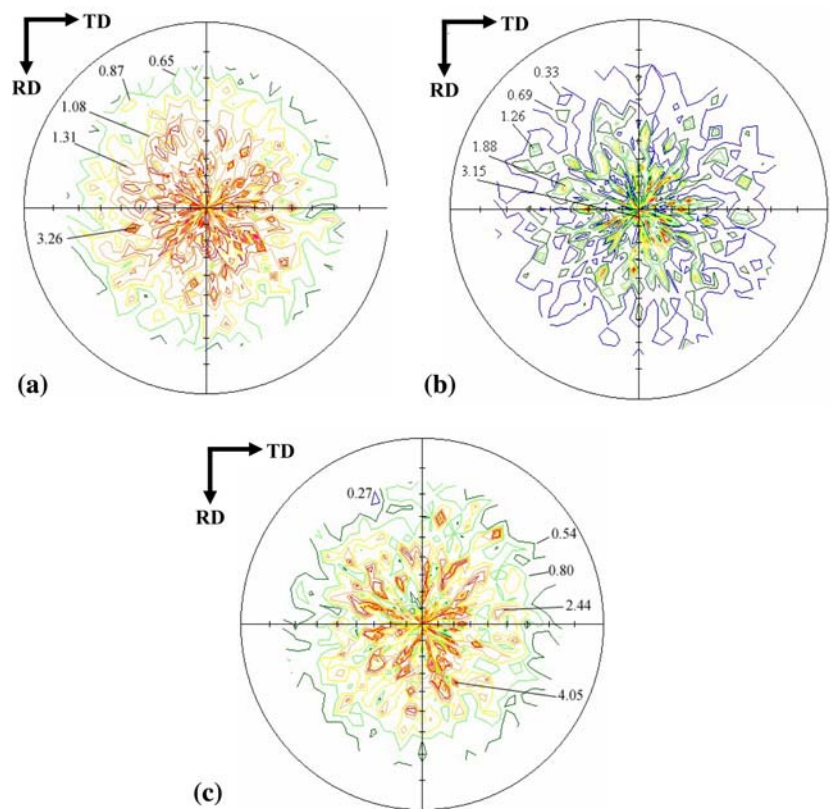


Table 2 Grain size in longitudinal and transversal sections of the steel plate

Section	EBSD				LOM		
	Area 1 Grain size (μm)	Area 2 Grain size (μm)	Area 3 Grain size (μm)	Number of sampled grains	Grain size (μm)	Random fields	Number of sampled grains
Longitudinal	38.8	40.6	40.9	293	50.5 ± 2.3	20	1,135
Transversal	62.4	51.9	60.1	277	59.3 ± 4.7	20	1,040

Fig. 3 {211} pole figure of the IF-steel plate obtained via XRD: (a) longitudinal section (rolling plane); (b) longitudinal section (mid-thickness); (c) transversal section. RD and TD refer, respectively, to the rolling and transversal directions



the thickness of the plate. These results are in agreement with those reported for hot-rolled extra-low-C- and IF steel plates [2–4, 10, 11].

Figures 4 and 5 show the OIM maps corresponding to two distinct regions obtained from EBSD data in the

longitudinal and transversal sections of the IF steel plate, respectively. For sake of clarity, two representative areas are shown in the present paper. In addition to the OIM maps, the results of the mesotexture corresponding to the mapped areas are also shown. It was observed that the

Fig. 4 OIM results of the longitudinal section of the IF steel plate (scan L3): (a) OIM map; (b) quality map of the OIM map with boundaries; (c) ODF with Euler angles ($\varphi_2 = 45^\circ$, Bunge notation)

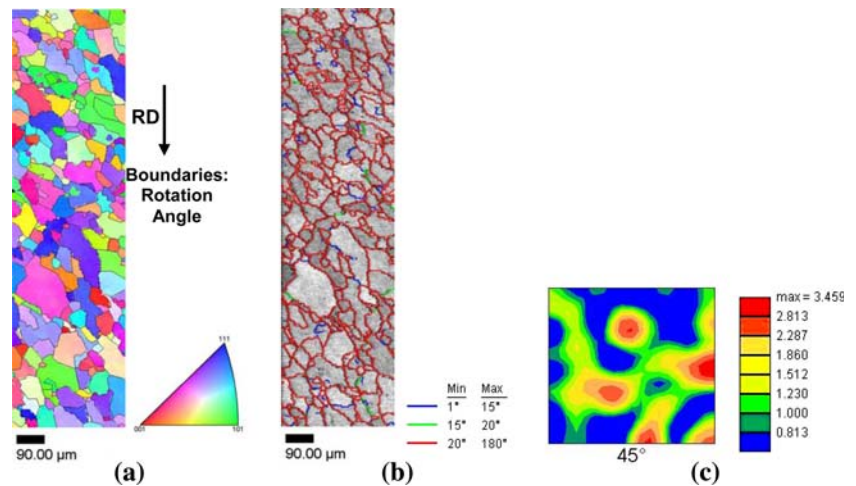
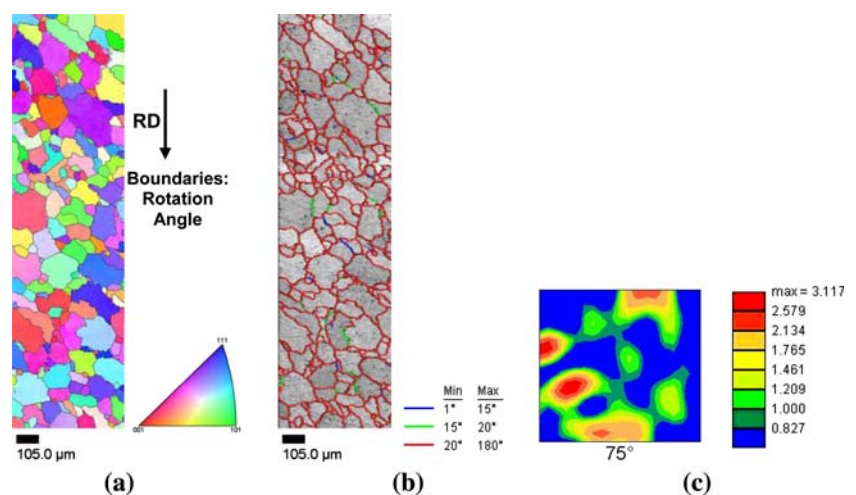


Fig. 5 OIM results of the transversal section of the IF steel plate (scan T1): (a) OIM map; (b) quality map of the OIM map with boundaries; (c) ODF with Euler angles ($\varphi_2 = 75^\circ$, Bunge notation)



average volume fraction of grain boundaries with low angle character ($2^\circ \leq \psi \leq 15^\circ$) is less than 5%. For this reason and other factors earlier discussed, we note a slight difference in the grain size results. As expected, the orientation distribution functions (ODF) differ significantly from one region to another. Tables 3 and 4 summarize the most intense orientation components found in every mapped area of the longitudinal and transversal sections, respectively. We also noted that some components like rotated cube ($\{001\}\langle 110 \rangle$) were very prominent in the orientation maps of the rolling plane. Ray et al. [3] reports that the rotated cube component arises primarily from the austenite-to-ferrite transformation following the Kurdjumov–Sachs orientation relationship. This kind of transformation is a strong evidence that an extended dynamic recrystallization process takes place during the hot rolling step because, if recrystallization in austenite does not occur during or after rolling, other strong orientation components like brass $\{110\}\langle 112 \rangle$, copper $\{112\}\langle 111 \rangle$, S $\{123\}\langle 634 \rangle$ and a weak Goss $\{110\}\langle 001 \rangle$ are developed [3].

Table 3 Microtexture results corresponding to the rolling plane of the IF steel plate obtained from OIM maps (L1, L2, and L3)

Component	(hkl)[uvw]	Intensity	φ_2	Scan
Main	(332)[1 $\bar{1}$ 0]	2.7	45°	L1
Secondary	(114)[$\bar{2}$ 21]	2.5		
	(114)[1 $\bar{1}$ 0]	2.5		
	(665)[0 $\bar{5}$ 6]	2.5		
Main	(334)[$\bar{2}$ 23]	3.4	45°	L2
Secondary	(110)[1 $\bar{1}$ 2]	2.9		
	(227)[106]	2.7		
	(665)[496]	2.9	45°	L3
Secondary	(001)[$\bar{2}$ 50]	2.8		
	(111)[$\bar{1}$ 23]	2.7		

The presence of subgrains in the ferrite microstructure, as shown by the TEM micrograph of Fig. 2b, can be explained by the relatively high transformation temperature of IF steels. Transformation-induced dislocations in ferrite

Table 4 Microtexture results corresponding to the transversal section of the initial IF steel plate obtained from OIM maps (T1, T2, and T3)

Component	(hkl)[uvw]	Intensity	ϕ_2	Scan
Main	(416)[1 $\bar{4}$ 0]	3.0	75°	T1
Secondary	(037)[205]	2.9		
Main	(001)[$\bar{1}\bar{1}$ 0]	3.6	90°	T2
Main	(774)[1 $\bar{1}$ 0]	4.3	45°	T3
Secondary	(220)[5 $\bar{8}$ 3]	3.5		

have been observed rather frequently [12], usually in the form of dislocation tangles [13]. Recovery processes due to relatively slow cooling rates (plate of 38 mm thickness) can then be expected to form subgrains. However, the resultant subgrain boundaries should have rather low misorientations (of the order of 1°), in contrast to the “low-angle grain boundaries” observed by EBSD with misorientations of 2–15°.

For the first time, evidences of the recovery in the microstructure of a hot-rolled Ti-stabilized IF steel are reported using traditional techniques of microstructural and textural characterization.

Conclusions

The microstructural and textural characterization of Ti-stabilized IF steel hot-rolled in the austenite range has been performed. A new and less hazardous methodology for metallography preparation of ultra-low carbon steels has also been presented. A good agreement between the results in terms of grain size determination provided by a LOM routine and the EBSD technique was found. The results showed the existence of a very weak and diffuse (nearly

random) texture in the hot-band resulting from the transformation of austenite into ferrite. The mesotexture analysis showed the presence of less than 5% of boundaries with low angle character ($2^\circ \leq \psi < 15^\circ$). The substructure also displayed a subgrain population. It can be concluded that these low angle boundaries and the presence of subgrains can be primarily associated to the existence of a few areas softened by recovery during or after hot rolling in austenitic field.

Acknowledgements The authors acknowledge the financial support provided by FAPESP and are grateful to IPEN (MSc. Marilene Serna) for the texture measurements, and to the Universidade de São Paulo (Dr.-Ing. A.F. Padilha) for allowing the use of the EBSD facilities. Thanks are due to Professor Paulo Rangel Rios (EEIMVR/UFF, Brazil) for going through the manuscript meticulously.

References

- Hutchinson WB (1984) *Int Met Rev* 29:25
- Hölscher M, Raabe D, Lücke K (1991) *Steel Res* 62:567
- Ray RK, Jonas JJ, Hook RE (1994) *Int Mater Rev* 39:129
- Jonas JJ (2001) *J Mater Proc Tec* 117:293
- Cross JJ, Randle V, Daniel SR (2000) *Mater Sci Tec* 16:1380
- Lins JFC, Sandim HRZ, Ribeiro RB, Pinto AL (2003) *Acta Microsc* 12:121
- Wright SI, Adams BL (1992) *Metall Trans* 23A:759
- Randle V, Dingley DJ (1992) *J Mater Sci* 27:4545
- Humphreys FJ (1999) *Mater Sci* 195:175
- Samjdar I, Verlinden B, Van Houtte P (1998) *Acta Mater* 46:2751
- Juntunen P, Raabe D, Karjalainen P, Kopio T, Bolle G (2001) *Metall Mater Trans* 32A:1989
- Honeycombe RWK (1985) In: Gray JM et al (ed) *Proceedings of international conference on “HSLA steels: metallurgy and applications”*. ASM, Beijing, Metals Park, OH, p 243
- Campos SS, Morales EV, Kestenbach H-J (2001) *Metall Mater Trans A* 32A:1245